Cage Compounds

International Edition: DOI: 10.1002/anie.201607681
German Edition: DOI: 10.1002/ange.201607681

Alleno-Acetylenic Cage (AAC) Receptors: Chiroptical Switching and Enantioselective Complexation of *trans*-1,2-Dimethylcyclohexane in a Diaxial Conformation

*Cornelius Gropp, Nils Trapp, and François Diederich**

In memory of Professor Vladimir Prelog

Abstract: *Four enantiopure 1,3-diethynylallenes (DEAs) with OH termini were attached to the rim of a resorcin[4]arene cavitand. The system undergoes conformational switching between a cage form, closed by a circular H-bonding array, and an open form, with the tertiary alcohol groups reaching outwards. The cage form is predominant in apolar solvents, and the open conformation in small, polar solvents. Both states were confirmed in solution and in X-ray co-crystal structures. ECD spectra of the alleno-acetylenic cages (AACs) are highly conformation sensitive, the longest wavelength Cotton effect at 304 nm switches from $\Delta\varepsilon = +191\,M^{-1}cm^{-1}$ for open $(P)_4$-AAC⊂acetonitrile to $\Delta\varepsilon = -691\,M^{-1}cm^{-1}$ ($\Delta\Delta\varepsilon = 882\,M^{-1}cm^{-1}$) for closed $(P)_4$-AAC⊂cyclohexane. Complete chiral resolution of (±)-trans-1,2-dimethylcyclohexane was found in the X-ray structures, with $(P)_4$-AAC exclusively bound to the (R,R)- and $(M)_4$-AAC to the (S,S)-guest. Guest inclusion occurs in a higher energy diaxial conformation.*

Molecular recognition studies have greatly advanced the understanding of enantioselective binding of chiral guests by natural and artificial host systems, establishing fundamental concepts, such as the three-point interaction model and Fischer's shape complementarity.[1] Cram et al. and Prelog et al. conducted early pioneering studies on the design of artificial crown ether receptors for chiral recognition.[2,3] As a result, chiral covalent container molecules and supramolecular, mainly hydrogen-bonded capsular assemblies were investigated to bind optically active guests in their defined inner phase.[4,5] Herein, we report the first enantioselective inclusion complex of a chiral alicyclic hydrocarbon—based purely on dispersive interactions and optimal space filling—by a capsular receptor closed by a circular hydrogen-bonding array. This receptor undergoes solvent-induced switching between an open and a closed state featuring dramatically different chiroptical properties.

Since the first successful report of their synthesis and chiral separation, enantiopure 1,3-diethynylallenes (DEA, Scheme 1) have been increasingly used as all-carbon building blocks with high configurational stability and unique chiroptical properties.[6] Following the construction and study of homochiral macrocycles and acyclic oligomers,[7] DEAs were recently also introduced into more complex supramolecular assemblies.[8] The ease of monitoring guest-induced chiroptical changes by electronic circular dichroism (ECD) stimulated us to combine the pronounced chiroptical features of the enantiopure alleno-acetylenes with receptor motifs for the development of chiral chemosensors.[8c,9–11]

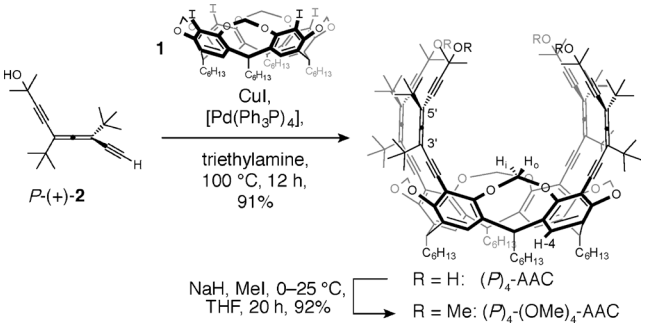

Scheme 1. Reagents and conditions for the synthesis of $(P)_4$-AAC from *P*-(+)-**2** and tetraiodo-cavitand **1**. Methylation of $(P)_4$-AAC yields $(P)_4$-$(OMe)_4$-AAC. $(M)_4$-configured AACs were obtained from (*M*)-(−)-**2**.

We selected the methylene-bridged tetraiodo-resorcin[4]arene cavitand **1** with *n*-hexyl legs as a concave platform to build the chiral receptors (Scheme 1).[4c,12,13] $(P)_4$-AAC was prepared by Sonogashira cross-coupling of **1** with enantiomerically pure DEA (*P*)-(+)-**2** (5.0 equiv)[14] in 91% yield (Scheme 1). Methylation of the tertiary alcohol termini gave $(P)_4$-$(OMe)_4$-AAC. The corresponding enantiopure, $(M)_4$-configured compounds were obtained in a similar fashion starting from (*M*)-(−)-**2** (see Section S2.3 and S2.4 in the Supporting Information).

X-ray co-crystal structures of AACs (see Section S6) revealed two well-defined conformations: a closed one and an open one (Figure 1 A,B). The closed conformation, as shown by crystals of $(P)_4$-AAC⊂cycloheptane, features the alleno-acetylenes oriented inwards with the tertiary alcohols converging in a circular hydrogen-bonding array.

In the open conformation, as shown by crystals of $(P)_4$-AAC⊂acetonitrile, the alleno-acetylenes are oriented outwards with the *tert*-butyl groups of the alleno-acetylenic backbone facing into the cavity, thereby limiting the available space for binding.

[*] C. Gropp, Dr. N. Trapp, Prof. Dr. F. Diederich
Laboratorium für Organische Chemie
ETH Zurich
Vladimir-Prelog-Weg 3, CH-8093 Zurich (Switzerland)
E-mail: diederich@org.chem.ethz.ch

Supporting information for this article can be found under: http://dx.doi.org/10.1002/anie.201607681.

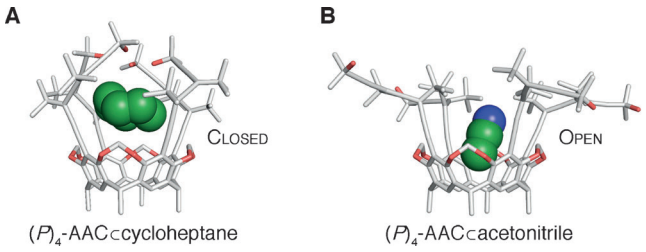

Figure 1. A) X-ray co-crystal structure of $(P)_4$-AAC⊂cycloheptane in the closed cage form. B) X-ray co-crystal structure of $(P)_4$-AAC⊂acetonitrile in the open conformation. Guests are shown in space-filling representation. Hydrogen atoms and *n*-hexyl alkyl chains are omitted for clarity.[24]

To confirm the presence of both conformations in solution, we studied the AACs by ^{1}H NMR, 2D ROESY NMR, and IR spectroscopies in various solvents. Larger apolar solvents were anticipated to stabilize the closed conformation, while small, polar solvents were expected to stabilize the open conformation through binding. A strong solvent-dependent chemical shift of the tertiary OH resonance of the AACs was observed in the ^{1}H NMR spectra. The OH resonance δ_{OH} shifted from $\delta = 2.4$ ppm in $CDCl_3$ to $\delta = 5.3$ ppm in [D_{12}]cyclohexane, in accordance with H-bonding in [D_{12}]cyclohexane (Section S3.2). Similarly, a large shift of the OH wavenumber $\tilde{\nu}_{OH}$ to lower energy was recorded in the IR spectra upon changing from dichloromethane ($\tilde{\nu} = 3600\ cm^{-1}$) to cyclohexane ($\tilde{\nu} = 3370\ cm^{-1}$) (Section S3.4). These spectral shifts confirm the formation of strong H-bonds in apolar solvents. 2D ROESY NMR experiments (Section S3.3) support the rigid and preorganized nature of the closed conformation by revealing through-space correlation of spatially proximate groups only present in the cage form. The solution studies confirm a binary system with two well-defined conformations.

As shape persistency and symmetry are known to have a large impact on ECD intensities, we expected AACs to show strong excitonic coupling of the alleno-acetylenic chromophores.[14] Indeed, ECD spectra of $(P)_4$-AAC in cyclohexane show very large Cotton effects of $\Delta\varepsilon = +700\ M^{-1}cm^{-1}$ at $\lambda = 214$ nm and $\Delta\varepsilon = -691\ M^{-1}cm^{-1}$ at $\lambda = 304$ nm (Figure 2 A). Changing the solvent from cyclohexane to acetonitrile inverts the Cotton effects with lower absolute value in intensities: $\Delta\varepsilon = -231\ M^{-1}cm^{-1}$ at $\lambda = 214$ nm and $\Delta\varepsilon = +191\ M^{-1}cm^{-1}$ at $\lambda = 304$ nm (Figure 2 A). As expected, the $(M)_4$-AAC enantiomer displays the mirror image ECD traces. The solvent-induced switching of the Cotton effect at $\lambda = 304$ nm results in the remarkable value of $\Delta\Delta\varepsilon =$

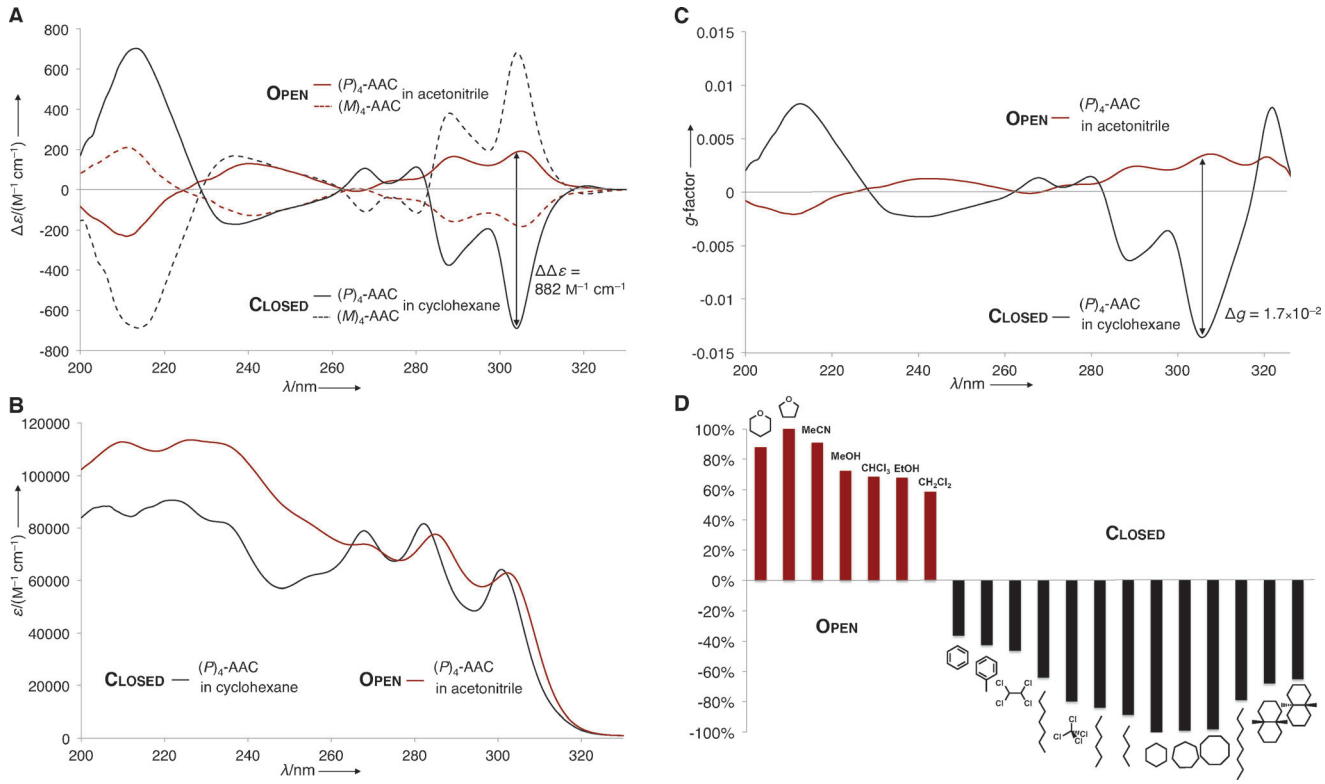

Figure 2. A) ECD spectra of $(P)_4$-AAC (solid lines) and $(M)_4$-AAC (dashed lines) at 293 K. Spectra in red display $(P)_4$-AAC and $(M)_4$-AAC in acetonitrile with $\Delta\varepsilon = -231\ M^{-1}cm^{-1}$ at $\lambda = 214$ nm and $\Delta\varepsilon = +191\ M^{-1}cm^{-1}$ at $\lambda = 304$ nm ($(P)_4$-enantiomer), spectra in black show $(P)_4$-AAC and $(M)_4$-AAC in cyclohexane with $\Delta\varepsilon = -700\ M^{-1}cm^{-1}$ at $\lambda = 214$ nm and $\Delta\varepsilon = +691\ M^{-1}cm^{-1}$ at $\lambda = 304$ nm ($(P)_4$-enantiomer). Switching between the open and closed conformation results in $\Delta\Delta\varepsilon = 882\ M^{-1}cm^{-1}$ at $\lambda = 304$ nm. B) UV/Vis spectra for $(P)_4$-AAC in acetonitrile (solid red line) and cyclohexane (solid black line) at 293 K (for additional data findings, see Figure S18). C) *g*-Factor plots for $(P)_4$-AAC in acetonitrile (solid red line) and cyclohexane (solid black line) with $\Delta g = 1.7\times10^{-2}$ at $\lambda = 304$ nm. D) Conformational excess (*CE*, %) of $(P)_4$-AAC in various solvents of different size and polarity determined on the basis of ECD intensities at $\lambda = 304$ nm and normalized to the strongest ECD intensity of each conformation (red: open conformation, tetrahydrofuran ($CE = +100\%$); black: closed conformation, cyclohexane ($CE = -100\%$)).

$882\,M^{-1}cm^{-1}$ between the complexes of the two conformers. The ECD signals of $(P)_4$-AAC and $(M)_4$-AAC are sensitive to temperature, showing enhanced signal intensities at lower temperatures (see Section S4.7). Importantly, the nature of the solvent had only a minimal effect on the absorption of non-polarized light, as revealed by UV/Vis spectroscopy (Figure 2B and Figure S21). A "monomeric" model system (2,6-dimethoxyphenyl-substituted DEAs *P*-**2** and *M*-**2**) served as comparison for solution studies and for the photophysical properties (see Section S2.5). The $\Delta\varepsilon_{max}$ intensities of the enantiopure AACs were around 100 times larger than those of the model systems, while the molar extinction coefficients (UV/Vis) of the AACs appeared to be the sum of contributions of four "monomeric" units (see Figures S15 and S16).

The contribution of the circular hydrogen-bonding array to the strong chiroptical properties was further analyzed in a comparison between $(P)_4$-AAC and its methylated analogue $(P)_4$-$(OMe)_4$-AAC. A very large difference of $\Delta\Delta\varepsilon = 623\,M^{-1}cm^{-1}$ was measured at $\lambda = 304$ nm in *n*-hexane (see Section S4.4). The methylated derivative cannot be switched into the closed state, underlining the importance of the circular hydrogen-bonding array for the cage formation and the exceptional chiroptical properties. The origin of the outstanding chiroptical properties was further studied by *g*-factor analysis, with *g* defined as the ratio between the molar circular dichroism $\Delta\varepsilon$ and the molar extinction coefficient ε. The AAC enantiomer shows a high Δg-factor value of 1.7×10^{-2} (cyclohexane→acetonitrile) at $\lambda = 304$ nm (Figure 2C).[7,8,15]

To further elucidate the nature of the conformational switching, the conformational excess (*CE*, %) of $(P)_4$-AAC in various solvents of different size and polarity was analyzed (Figure 2D). For this purpose, the ECD absorption of $(P)_4$-AAC at $\lambda = 304$ nm in cyclohexane for the closed cage conformation, and in tetrahydrofuran for the open conformation, were defined as maximum ($CE = -100\,\%$ and $+100\,\%$, respectively). Large apolar solvents, such as *n*-octane, stabilize predominantly the closed cage conformations (CE_{closed}, $-79\,\%$), while small, more-polar solvents, such as methanol, stabilize the open conformation (CE_{open}, $+72\,\%$, Figure 2D and Figures S18–S20).[16] The predominant conformation in solution appears to be determined both by solvent size and bulk properties, in agreement with binding to the closed or open form. To further substantiate the effect of the solvent size on the conformational switching, we compared $(P)_4$-AAC and $(P)_4$-$(OMe)_4$-AAC in different solvents of varying size (see Section S4.6). For solvents with similar bulk properties but differing in size, such as dichloromethane and tetrachloroethane, a switch from the open to the closed state is observed for $(P)_4$-AAC ($\Delta\Delta\varepsilon = 453\,M^{-1}cm^{-1}$ at $\lambda =$ 304 nm, see Figure S25). We conclude from these experiments, that shape complementarity and structural preorganization of the solvent has a major influence on the host conformation and chiroptical properties in solution.

In host–guest complexation studies, we were particularly interested in the recognition of pure hydrocarbons for which host–guest interactions solely rely on relatively weak dispersive interactions and C–H···π contacts. The absence of strong directional interactions, such as H-bonding, allowed the potential of AACs to be explored as chiral receptors based solely on these interactions and shape complementarity. Methods to obtain single crystals of solid-state inclusion complexes suitable for X-ray diffraction were developed (see Section S6). Seven X-ray co-crystal structures with different guests were obtained, five of which are highlighted in Figure 3 (for all co-crystal-structures, see Section S6). The co-crystal structures of $(P)_4$-AAC (Figure 3A–D) reveal an interesting feature, as the receptor adjusts the size and shape of the cavity based on the guest. For guests, such as cyclohexane (A) and methylcyclohexane (B), the host compensates for the missing shape complementarity by rotating one of the methyl groups of the tertiary alcohol termini into the cavity (highlighted as a blue ball, Figures 3A,B). By introducing an additional methyl group, such as in *cis*- and (±)-*trans*-1,2-dimethylcylohexane, the guest properly fills the cavity and all methyl groups of the H-bonded alcohol groups are now facing away from the cavity (Figures 3C,D). For evaluation of the adaptable nature of the host to optimize space-filling and dispersive interactions, we calculated the packing coefficients (*PC*, ratio of guest volume to host cavity volume) of each guest (see Section S7) from X-ray data. Upon changing from methylcyclohexane to *cis*- or (±)-*trans*-1,2-dimethylcyclohexane, the cavity size increases by 14% ($190\,Å^3 \rightarrow 220\,Å^3$) maintaining the optimal packing coefficient of approximately 55% as defined by Mecozzi and Rebek.[17]

It was long postulated that the enantiomeric conformers of *cis*-1,2-dimethylcyclohexane, which at room temperature rapidly interconvert via an achiral transition state yielding an overall achiral molecule, could be resolved at low temperatures (ca. −150 °C), yet this has never been reported experimentally.[18] The X-ray co-crystal structure of $(P)_4$-AAC⊂*cis*-1,2-dimethylcyclohexane shows two equally populated (50:50%) occupancies of the guest, which correspond to the two enantiomers (Figure 3C). This is the first experimental observation of both enantiomers of *cis*-1,2-dimethylcyclohexane in the solid state at low temperatures (measured at 100 K).[19] No X-ray crystal structure of this compound had previously been reported. The *gauche* torsional angles Me-C(1)-C(2)-Me in both enantiomeric conformers are −67.8 and +57.7°, respectively (for further details of the guest conformation, see Section S6.7).

Compared to the *cis* isomer, the enantiomers of (±)-*trans*-1,2-dimethylcyclohexane are stable and not interconvertable at room temperature. Each enantiomer has two conformers, the more stable diequatorial and the less stable diaxial (Figure 3D). The difference in Gibbs energy ($\Delta\Delta G^0_{298\,K}$) between the two conformations had been determined to be 2.74 kcal mol^{-1}.[18b,c] To study the enantioselective binding potential of the AACs, crystallization experiments of the two enantiopure $(P)_4$- and $(M)_4$-AACs with the racemic mixture of (±)-1,2-*trans*-dimethylcyclohexane were set up (see Section S6.5). While $(P)_4$-AAC crystallized selectively with encapsulated (*R*,*R*)-*trans*-1,2-dimethylcyclohexane, $(M)_4$-AAC showed complete selectivity for the (*S*,*S*)-enantiomer. Even more intriguing was the finding that the higher-energy diaxial conformer of (*R*,*R*)-*trans*-1,2-dimethylcyclohexane and (*S*,*S*)-*trans*-1,2-dimethylcyclohexane crystallized with $(P)_4$-AAC and $(M)_4$-AAC, respectively, an unprecedented

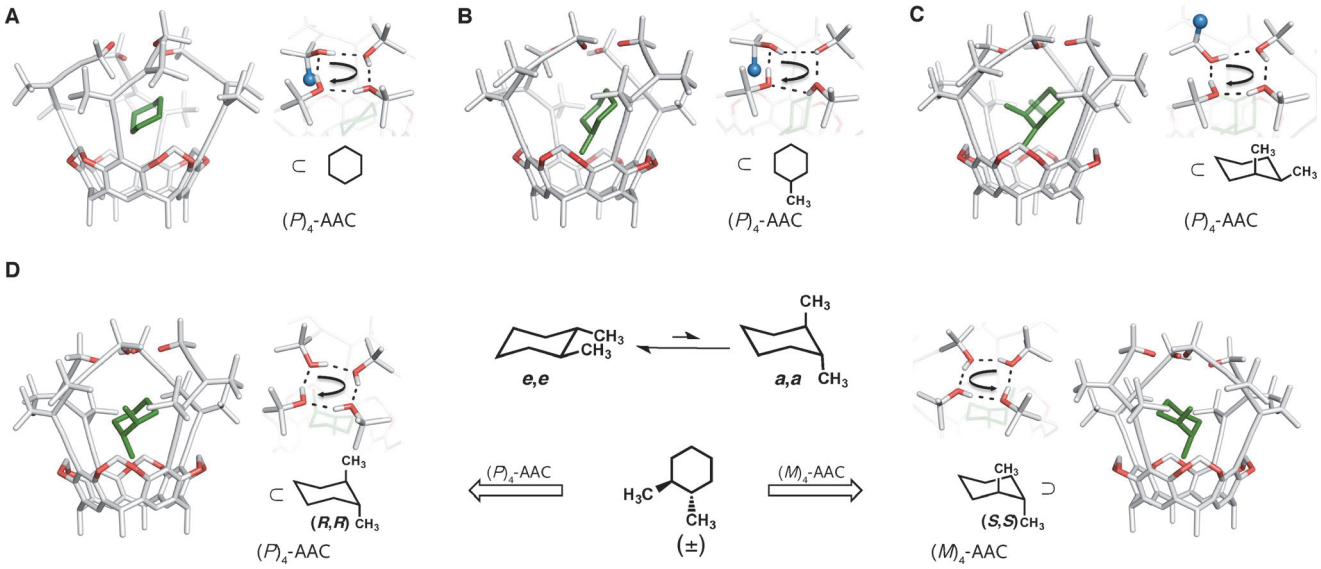

Figure 3. A–D) X-ray co-crystal structures of $(P)_4$-AAC⊂guest and $(M)_4$-AAC⊂guest (guests: cyclohexane (A), methylcyclohexane (B), *cis*-1,2-dimethylcyclohexane (C), and enantiomers of *trans*-1,2-dimethylcyclohexane in a diaxial conformation (D)).[24] The fourfold circular hydrogen-bonding array is shown for all complexes. Depending on the size of the guest, the AACs compensate for the missing space filling of the guest by rotating one methyl group into the cavity (highlighted as a blue ball in A–C). In structures A, C, and D, all hydrogen atoms could be resolved crystallographically. In all structures of $(P)_4$-AAC (Figure 3 D, left), the circular hydrogen-bonding array follows a clockwise orientation. For $(M)_4$-AAC (Figure 3 D, right), the hydrogen-bonding array follows a counter-clockwise orientation. D) Left: Chiral recognition of (*R*,*R*)-*trans*-1,2-dimethylcyclohexane in a diaxial conformation by $(P)_4$-AAC. Right: Chiral recognition of (*S*,*S*)-*trans*-1,2-dimethylcyclohexane in a diaxial conformation by $(M)_4$-AAC.[18].

observation. The guest molecules are in the chair conformation with both methyl groups approaching a *trans*-diaxial alignment. The dihedral angles (Me-C(1)-C(2)-Me) correspond to −148° for the (*R*,*R*)-guest and +144° for the (*S*,*S*)-guest (Table S23).[20] This deviation from the perfect diaxial conformation (180°) together with substantial bond-length and bond-angle alteration in the carbon scaffold seems to reduce the strain caused by the 1,3-diaxial interactions in the bound molecule. No particularly repulsive host–guest contacts (heavy atom distances below 3.4 Å) are observed in the crystals. The detailed conformation of the two bound enantiomers is reported in Section S6.6. The data suggest the need for new conformational analysis of the *trans*-1,2-dimethylcyclohexane at the highest level of theory.[21]

The enantioselectivity and the preference for the inclusion of the diaxial conformer are remarkable in the absence of directional interactions and are both due to the structural rigidity and preorganization of the cage and its interior volume. This rigidity is induced by the circular fourfold hydrogen-bonding array. $(P)_4$-configured AACs show a clockwise orientation of this hydrogen-bonding array, while the $(M)_4$-configured AACs display a counter-clockwise orientation (see Figure 3 and Section S6.3). The fixed orientation of the hydrogen-bonding array, present in the solid state, appears to be dictated by the $(P)_4$- or $(M)_4$-configuration of the AACs.[22] This handedness of the H-bonding interaction stabilizes the cage form of the receptor and makes a key contribution to both the outstanding chiroptical properties and the excellent enantioselectivity in binding.

The encapsulation of guests was also investigated in solution. Conformation-dependent binding studies by ^{1}H NMR and ECD titrations targeting either the closed conformation with *n*-octane or the open conformation with methanol as a solvent were performed (see Figure 2 D and Figure S27). *n*-Octane, which competes with the added guest for the capsular binding cavity, was chosen over the bulky mesitylene, which is a non-competitive solvent. Both solvents give comparable apparent binding constants (see Table S18), but *n*-octane has the advantage of being UV/Vis transparent (Table 1). The apparent binding constants (K_{app}) for guests,

Table 1: Apparent binding constants (K_{app}) at 293 K for various guests by $(P)_4$-AAC in the open and closed conformation.

Guest	ECD[a] K_{app} [M^{-1}]	ECD[b] $\Delta G_{293\,K}$ [kcal mol^{-1}]
in n-octane: closed conformation		
Cycloheptane	141	−2.9
Methylcyclohexane	22	−1.8
cis-1,2-Dimethylcyclohexane	347	−3.4
(±)-*trans*-1,2-Dimethylcyclohexane	107[23]	−2.7
in methanol: open conformation		
Cyclopentane	6	−1.0
Methylcyclopentane	8	−1.2
Triisopropylsilylacetylene	19	−1.7

[a] The apparent binding constant K_{app} was determined by non-linear least-square curve fitting of ECD intensities at λ = 304 nm, assuming 1:1 binding (see Section S5). The overall error was estimated to be in the range of 20%. [b] The Gibbs binding energy was calculated from $K_{app\,293\,K}$. For comparison of K_{app} by ECD and ^{1}H NMR spectroscopy, see Section S5.3.

which are not corrected for solvent competition and host dimerization, were obtained by non-linear least-square fitting of both ECD titrations and ^{1}H NMR titrations at fast host–guest exchange. As a general note, the ECD titrations have much higher accuracy and provide more reliable data, since large changes in band intensity are recorded in all titrations, while the observed changes in chemical shifts in the ^{1}H NMR titrations are small and therefore more error-prone (see Table S18). In methanol as a weakly competitive solvent, $(P)_4$-AAC in the open form gave $K_{app} = 6–19\,M^{-1}$ for the weak complexation of small guests (Table 1, for titration curves see Section S5); both NMR and ECD methods gave similar values. The binding of alicyclic hydrocarbon guests by the closed cage form in *n*-octane is significantly stronger by over one order of magnitude. In *n*-octane, methylcyclohexane binds with $K_{app} = 22\,M^{-1}$. Cycloheptane ($K_{app} = 141\,M^{-1}$) and *cis*-1,2-dimethylcyclohexane ($K_{app} = 341\,M^{-1}$) show higher binding constants while the complexation of (±)-*trans*-1,2-dimethylcyclohexane ($K_{app} = 107\,M^{-1}$) is weaker because of the investment of binding energy to access the higher energy diaxial conformation.[23] A difference in binding constants for complexes of the closed form by a factor of approximately 2 is obtained by ^{1}H NMR (lower K_{app}) and ECD titrations (Table S18) in deuterated and non-deuterated *n*-octane, respectively, and was explained by self-dimerization of $(P)_4$-AAC (see Section S5.4), which is more competitive in the higher concentration ranges of the ^{1}H NMR titrations.

In summary, we present a comprehensive and systematic study of alleno-acetylenic cages undergoing solvent-dependent binary conformational switching between a closed cage form, stabilized by a circular fourfold H-bonding array, and an open state. The two conformations differ extremely in their chiroptical properties, with $\Delta\Delta\varepsilon$ values of up to $882\,M^{-1}cm^{-1}$ at $\lambda = 304$ nm when changing from acetonitrile to cyclohexane. X-ray co-crystal structures show that $(P)_4$-configured AACs dictate a clockwise orientation of the circular H-bonding array, while $(M)_4$-configured AACs display a counter-clockwise orientation. This directionality of the circular H-bonding pattern enhances the chiroptical and chiral recognition properties of the cage form. In complexation studies with cycloalkanes, $(P)_4$-AAC and $(M)_4$-AAC feature complete chiral resolution in the solid state, with enantioselective binding of (*R*,*R*)-1,2-*trans*-dimethylcyclohexane by the $(P)_4$-cage and of (*S*,*S*)-*trans*-1,2-dimethylcyclohexane by the $(M)_4$-cage. Remarkably, the enantiomers bind in a higher energy diaxial conformation. This example of a highly confined enantiopure cage receptor with outstanding chiral recognition properties opens numerous possibilities in chiral separation, catalysis, and extensive further molecular recognition studies.

Acknowledgements

This work was supported by a grant from the Swiss National Science Foundation. C.G. was supported by the Studienstiftung des Deutschen Volkes. We thank René Arnold and Dr. Marc-Olivier Ebert for recording 2D NMR spectra, Michael Solar for measuring X-ray crystal structures, and Dr. Bruno Bernet, Dr. Oliver Dumele, and Anatol Schwab for valuable comments on the manuscript.

Keywords: alleno-acetylenes · cage compounds · chiral recognition · chiroptical chemosensor · supramolecular chemistry

[1] a) E. Fischer, *Ber. Dtsch. Chem. Ges.* **1894**, *27*, 2985–2993; b) L. H. Easson, E. Stedman, *Biochem. J.* **1933**, *27*, 1257–1266.
[2] a) D. J. Cram, J. M. Cram, *Acc. Chem. Res.* **1978**, *11*, 8–14; b) D. J. Cram, K. N. Trueblood, *Top. Curr. Chem.* **1981**, *98*, 43–106.
[3] a) V. Prelog, *Pure Appl. Chem.* **1978**, *50*, 893–904; b) V. Prelog, S. Mutak, *Helv. Chim. Acta* **1983**, *66*, 2274–2278.
[4] a) J. Canceill, L. Lacombe, A. Collet, *J. Am. Chem. Soc.* **1985**, *107*, 6993–6996; b) J. K. Judice, D. J. Cram, *J. Am. Chem. Soc.* **1991**, *113*, 2790–2791; c) D. J. Cram, J. M. Cram, *Container molecules and their guests*, Royal Society of Chemistry, Cambridge, **1997**; d) J. Yoon, D. J. Cram, *J. Am. Chem. Soc.* **1997**, *119*, 11796–11806; e) T. Brotin, L. Guy, A. Martinez, J.-P. Dutasta, *Top. Curr. Chem.* **2013**, *341*, 177–230; f) D. Zhang, J.-C. Mulatier, J. R. Cochrane, L. Guy, G. Gao, J.-P. Dutasta, A. Martinez, *Chem. Eur. J.* **2016**, *22*, 8038–8042.
[5] a) M. M. Conn, J. Rebek, Jr., *Chem. Rev.* **1997**, *97*, 1647–1668; b) E. E. Simanek, S. Qiao, I. S. Choi, G. M. Whitesides, *J. Org. Chem.* **1997**, *62*, 2619–2621; c) L. R. MacGillivray, J. L. Atwood, *Nature* **1997**, *389*, 469–472; d) J. M. Rivera, T. Martín, J. Rebek, Jr., *Science* **1998**, *279*, 1021–1023; e) R. K. Castellano, C. Nuckolls, J. Rebek, Jr., *J. Am. Chem. Soc.* **1999**, *121*, 11156–11163; f) J. M. Rivera, J. Rebek, Jr., *J. Am. Chem. Soc.* **2000**, *122*, 7811–7812; g) J. M. Rivera, S. L. Craig, T. Martín, J. Rebek, Jr., *Angew. Chem. Int. Ed.* **2000**, *39*, 2130–2132; *Angew. Chem.* **2000**, *112*, 2214–2216; h) J. J. González, R. Ferdani, E. Albertini, J. M. Blasco, A. Arduini, A. Pochini, P. Prados, J. de Mendoza, *Chem. Eur. J.* **2000**, *6*, 73–80; i) F. Hof, S. L. Craig, C. Nuckolls, J. Rebek, Jr., *Angew. Chem. Int. Ed.* **2002**, *41*, 1488–1508; *Angew. Chem.* **2002**, *114*, 1556–1578; j) J. L. Atwood, A. Szumna, *J. Am. Chem. Soc.* **2002**, *124*, 10646–10647; k) A. Scarso, A. Shivanyuk, O. Hayashida, J. Rebek, Jr., *J. Am. Chem. Soc.* **2003**, *125*, 6239–6243; l) A. Galan, P. Ballester, *Chem. Soc. Rev.* **2016**, *45*, 1720–1737.
[6] a) R. C. Livingston, L. R. Cox, V. Gramlich, F. Diederich, *Angew. Chem. Int. Ed.* **2001**, *40*, 2334–2337; *Angew. Chem.* **2001**, *113*, 2396–2399; b) R. Livingston, L. R. Cox, S. Odermatt, F. Diederich, *Helv. Chim. Acta* **2002**, *85*, 3052–3077; c) J. L. Alonso-Gómez, P. Schanen, P. Rivera-Fuentes, P. Seiler, F. Diederich, *Chem. Eur. J.* **2008**, *14*, 10564–10568.
[7] a) J. L. Alonso-Gómez, P. Rivera-Fuentes, N. Harada, N. Berova, F. Diederich, *Angew. Chem. Int. Ed.* **2009**, *48*, 5545–5548; *Angew. Chem.* **2009**, *121*, 5653–5656; b) P. Rivera-Fuentes, J. L. Alonso-Gómez, A. G. Petrovic, F. Santoro, N. Harada, N. Berova, F. Diederich, *Angew. Chem. Int. Ed.* **2010**, *49*, 2247–2250; *Angew. Chem.* **2010**, *122*, 2296–2300; c) P. Rivera-Fuentes, J. L. Aonso-Gómez, A. G. Petrovic, P. Seiler, F. Santoro, N. Harada, N. Berova, H. S. Rzepa, F. Diederich, *Chem. Eur. J.* **2010**, *16*, 9796–9807; d) E. J. Donckele, O. Gidron, N. Trapp, F. Diederich, *Chem. Eur. J.* **2014**, *20*, 9558–9566.
[8] a) M. D. Tzirakis, N. Marion, W. B. Schweizer, F. Diederich, *Chem. Commun.* **2013**, *49*, 7605–7607; b) M. D. Tzirakis, M. N. Alberti, H. Weissman, B. Rybtchinski, F. Diederich, *Chem. Eur. J.* **2014**, *20*, 16070–16073; c) O. Gidron, M.-O. Ebert, N. Trapp, F. Diederich, *Angew. Chem. Int. Ed.* **2014**, *53*, 13614–13618; *Angew. Chem.* **2014**, *126*, 13833–13837; d) O. Gidron, M.

Jirásek, N. Trapp, M.-O. Ebert, X. Zhang, F. Diederich, *J. Am. Chem. Soc.* **2015**, *137*, 12502 – 12505.
[9] a) G. A. Hembury, V. V. Borovkov, Y. Inoue, *Chem. Rev.* **2008**, *108*, 1 – 73; b) G. Pescitelli, L. Di Bari, N. Berova, *Chem. Soc. Rev.* **2011**, *40*, 4603 – 4625; c) C. Wolf, K. W. Bentley, *Chem. Soc. Rev.* **2013**, *42*, 5408 – 5424; d) G. Pescitelli, L. Bari, N. Berova, *Chem. Soc. Rev.* **2014**, *43*, 5211 – 5233.
[10] S. Míguez-Lago, A. L. Llamas-Saiz, M. M. Cid, J. L. Alonso-Gómez, *Chem. Eur. J.* **2015**, *21*, 18085 – 18088.
[11] P. Rivera-Fuentes, F. Diederich, *Angew. Chem. Int. Ed.* **2012**, *51*, 2818 – 2828; *Angew. Chem.* **2012**, *124*, 2872 – 2882.
[12] F. Gruppi, F. Boccini, L. Elviri, E. Dalcanale, *Tetrahedron* **2009**, *65*, 7289 – 7295.
[13] L. Sebo, F. Diederich, V. Gramlich, *Helv. Chim. Acta* **2000**, *83*, 93 – 113.
[14] P. Rivera-Fuentes, B. Nieto-Ortega, W. B. Schweizer, J. T. L. Navarrete, J. Casado, F. Diederich, *Chem. Eur. J.* **2011**, *17*, 3876 – 3885.
[15] a) H. Langhals, J. Gold, *Liebigs Ann.* **1997**, 1151 – 1153; b) R. S. Walters, C. M. Kraml, N. Byrne, D. M. Ho, Q. Qin, F. J. Coughlin, S. Bernhard, R. A. Pascal, Jr. *J. Am. Chem. Soc.* **2008**, *130*, 16435 – 16441.
[16] We conducted low-temperature ^{1}H NMR experiments of $(P)_4$-AAC in [D_8]toluene ($CE = -43\,\%$). At low temperatures, (215 K) both conformations become distinguishable on the NMR timescale (see SI Figure S20).
[17] S. Mecozzi, J. Rebek, Jr., *Chem. Eur. J.* **1998**, *4*, 1016 – 1022.
[18] a) H. Booth, T. B. Grindley, *J. Chem. Soc. Chem. Commun.* **1983**, 1013 – 1014; b) M. Manoharan, E. L. Eliel, *Tetrahedron Lett.* **1983**, *24*, 453 – 456; c) E. L. Eliel, S. H. Wilen, L. N. Mander, *Stereochemistry of Organic Compounds*, John Wiley & Sons, Inc., New York, **1994**, pp. 702 – 703; the difference in Gibbs energy ($\Delta\Delta G^0_{298\,K}$) between the two conformations had been determined as 2.74 kcal mol^{-1}.
[19] Y. Inokuma, S. Yoshioka, J. Ariyoshi, T. Arai, Y. Hitora, K. Takada, S. Matsunaga, K. Rissanen, M. Fujita, *Nature* **2013**, *495*, 461 – 466.
[20] The dihedral angle (Me-C(1)-C(2)-Me) of (±)-*trans*-1,2-dimethylcyclohexane in the chair conformation with the methyl groups in the diequatorial orientation corresponds to −58°; R. Bream, D. Watkin, A. Cowley, *Acta Crystallogr., Sect. E* **2006**, *62*, o785 – o787.
[21] a) V. G. S. Box, L. L. Box, *J. Mol. Struct.* **2003**, *649*, 117 – 132; b) for distortions from perfectly axial conformations in calculated transition states of dioxirane C–H oxidations in methylated cyclohexanes, see: L. Zou, R. S. Paton, A. Eschenmoser, T. R. Newhouse, P. S. Baran, K. N. Houk, *J. Org. Chem.* **2013**, *78*, 4037 – 4048.
[22] An interesting finding in recent years of comparable achiral systems undergoing cyclic hydrogen-bonding networks was the simultaneous tunneling of protons in the solid state at low temperatures. We are currently investigating the effect of chirality towards the tunneling behavior; see a) D. F. Brougham, R. Caciuffo, A. J. Horsewill, *Nature* **1999**, *397*, 241 – 243; b) K. Ueda, M. Oguni, *J. Phys. Chem. B* **2012**, *116*, 14470 – 14476; c) K. Ueda, M. Oguni, *J. Phys. Chem. B* **2013**, *117*, 14157 – 14162; d) J. Meisner, J. Kästner, *Angew. Chem. Int. Ed.* **2016**, *55*, 5400 – 5413; *Angew. Chem.* **2016**, *128*, 5488 – 5502.
[23] Binding of (±)-*trans*-1,2-dimethylcyclohexane with $(M)_4$-AAC gave a similar value to that obtained with $(P)_4$-AAC (Table 1): $K_{app} = 148\,M^{-1}$ by ECD.
[24] CCDC 1496457—1496463 ($(P)_4$-AAC⊂Guest), contain the supplementary crystallographic data for this paper. These data can be obtained free of charge from The Cambridge Crystallographic Data Centre via The Cambridge Crystallographic Data Centre.

Received: August 8, 2016
Published online: ■■ ■■, ■■■■

Communications

Cage Compounds

C. Gropp, N. Trapp,
F. Diederich* ——— ■■■■–■■■■

Alleno-Acetylenic Cage (AAC) Receptors: Chiroptical Switching and Enantioselective Complexation of *trans*-1,2-Dimethylcyclohexane in a Diaxial Conformation

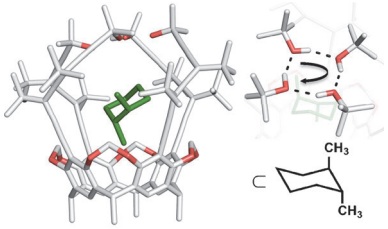

HIGHER-ENERGY CONFORMER BINDING & CHIRAL RECOGNITION

Enantioselective complexation: Enantiopure alleno-acetylenic cages show solvent-dependent binary conformational switching with dramatic differences in the chiroptical properties of the open and closed form. Complete chiral resolution of (±)-*trans*-1,2-dimethylcyclohexane is observed in X-ray co-crystal structures of the cage form. Inclusion complexation occurs in a higher-energy diaxial conformation of the guest.